

Determination of Material Properties for Welding Models by Means of Arc Weld Experiments

Phillip W. Fuerschbach
G. Richard Eisler
Sandia National Laboratories
Albuquerque, New Mexico.
<http://www.sandia.gov/soar/>

Abstract

Moving heat source solutions to the conduction heat flow equation are used to estimate the thermal diffusivity and thermal conductivity of nine engineering alloys. A technique is developed using gas tungsten arc edge weld data that enables least square fitting of the experimental weld size and heating parameters to the 2D and 3D conduction heat flow equations. Effective values of the thermal diffusivity and thermal conductivity are determined. Dimensionless parameters for the 2D and 3D solutions are given that correlate well with the experimental data and the weld theory. Property estimates for several 304 stainless steel weld experiments indicate the method yields property variations with an uncertainty of 11.1%. The experimental results are intended for welding software models to enable prediction of weld effects on the production floor.

Introduction

Manufacturers and designers often face challenging welding questions such as: What is the maximum temperature that will occur in a part just a few millimeters adjacent to the weld? What is the effect of a change to a new material on a qualified weld procedure? At what speed can a laser make full penetration welds on a new material for a production line? In general, intuition and experience are of little help when dealing with a complex non-linear process like fusion welding. Instead, the answers are usually determined through costly test, re-test, and analysis.

Despite the demonstrated success of conduction heat flow models in predicting fusion weld size, base metal temperatures, and processing requirements, weld model application in the manufacturing world is still uncommon.

Clearly, there are significant simplifications in these models since heat source dimensions, latent heat effects, workpiece energy losses, and weld pool convection are all ignored. Although the conduction models do not incorporate

these effects, the global heating of the sample is a strong indicator of the degree of melting which occurs, and in most cases, a conduction model can provide results no more uncertain than much more sophisticated analytical approaches.

The model simplifications have not decreased their value and application; the primary reason they are not used is simply a lack of the required thermal property values for most practical engineering alloys. Conduction heat flow models assume that the thermal properties are constant. Unfortunately this is not the case and both thermal conductivity and thermal diffusivity can vary significantly between room temperature and the liquidus temperature. The selection of one value over another or simply choosing an average value is a common approach to fit real experimental data to these models. Finding the correct values is a formidable task.

It seems logical that the best way to obtain the required property values for the conduction models is to make welds that exhibit the actual physical process characteristics.¹ This task is not as arduous as it may first appear. By carefully choosing weld sample dimensions we can readily simulate 2D or 3D heat flow. Input power and travel speed are easily measured for each weld, and the arc efficiency for gas tungsten arc welds is well known and very constant.²

Metallography allows us to readily observe the extent of the fusion zone and the overall volume. Certainly, variations in fusion zone dimensions due to convective currents will lead to significant discrepancies between the conduction model and actual weld dimensions. By fitting the conduction models to the measured weld pool cross-sectional area we can mitigate the uncertainty of the weld pool dimensions and yield a better fit as well as more accurate predictions of the global temperature fields around the fusion zone.

Experimental

The GTA edge welds for this experiment were made on thin (1.0 – 2.0 mm) sheet metal specimens of 304 stainless steel, Hastelloy B2, Hastelloy C4, Hastelloy C22, Kovar, 6061

Aluminum, and 1100 Aluminum. Samples were cleaned with alcohol prior to welding. Some weld data was taken from an earlier study on edge welds,² and some thick plate data was taken from the open literature.^{3,4}

Welds were made with a Weldlogic AWS 100 GTA power supply, with a Weldcraft WP27 air cooled GTA torch fitted with a 0.094 in diameter, 2% lanthanated electrode ground to a 60 degree tip angle. All welds were shielded with argon through a gas lens at 25 CFH. Arc gap was kept constant at 1.25 mm. All welds (including those made on aluminum) were made in the constant current mode with the electrode negative. For the aluminum welds, the aluminum oxide was removed prior to welding by scraping the edge weld surface with a knife.

A high speed digital oscilloscope recorded both the arc current and voltage signals, which when multiplied together yielded the actual arc power. Net input power was determined from the product of the average of the arc power waveform and a constant arc efficiency value of 0.80. For the higher arc power welds taken from the open literature⁴, a 0.75 arc efficiency value was used. Cross-sectional area measurements were taken from the average of four metallographic cross-sections for each sample.

For cases where previous experimental data was not employed, at least six welds including one replicate were made according to the experimental matrix shown in Fig. 1. Arc power and travel speed conditions were chosen to provide as large a range as practical. The limits of melting were bounded by the sample dimensions. The minimum amount of melting was established when the fusion zone just covered the top of the edge weld sample. The maximum amount of melting was established when the fusion zone became so large that it expanded significantly beyond the edges of the sample. Screening welds were made in order to find a slow speed and high current condition for maximum melting, as well as a fast speed and low current condition for the minimum melting condition.

The edge weld geometry constrained heat flow to two dimensions and allowed the moving line source solution for steady state conduction heat flow (1) to be used to determine the material properties.

Non-Linear Solve Description. Effective values of thermal conductivity (k) and thermal diffusivity (α) were calculated using Rosenthal's⁵ moving heat source solutions (1) and (2) to the conduction heat flow theory, where T is the melting temperature (for the melt contour), r is the resultant distance to a point on the melt contour from the origin, and x is the component in the direction opposite to the movement of the heat source (where $r^2 = x^2 + y^2$, y being the lateral coordinate). K_0 is the Bessel function of order 0.

$$\frac{2\pi(T - T_0)kt}{q_i} = e^{\left(\frac{vx}{2\alpha}\right)} K_0\left(\frac{vr}{2\alpha}\right) \quad (1)$$

$$\frac{2\pi(T - T_0)kr}{q_i} = e^{-\left(\frac{v}{2\alpha}(r-x)\right)} \quad (2)$$

Measured cross-sectional weld pool area (A) data for each material were least-squared fit with the experimental values of input power (q_i) and travel speed (v). The "fit" parameter was thermal diffusivity (α). In order to yield thermal property values that are realistic in magnitude, it was decided that "best available" values of the liquidus temperature (T_l) and the melt enthalpy (δh) (including the latent heat of fusion) would be used in the fitting equation.⁶

The relationship among the four thermal properties is given in (3). One can see from (3) that by specifying ΔT and δh , the thermal conductivity (k) is obtained directly from the thermal diffusivity fit result.

$$\alpha = \frac{k(T_l - T_o)}{\delta h} \quad (3)$$

T_o is the base metal temperature and was set at 23°C for all welds.

For both the 2-D line source and the 3-D semi-infinite plate welds, the equations were solved to yield the surface melt contour coordinates. Both solutions necessitated nonlinear algebraic solutions to resolve the coordinates, since ΔT , q_i , and v were all specified. The maximum width coordinate, w_{max} on the melt contour was assumed paired with the "penetration" coordinate. In the 2-D case the plate thickness, t , was taken as one half the width across the welded edge. The cross-sectional area was assumed rectangular, and the modeled area was therefore $w_{max} * t$. In the 3-D case, cross-sectional area was assumed semicircular, the penetration was considered to be $w_{max} / 2$, and therefore the modeled area was $\pi w_{max}^2 / 4$.

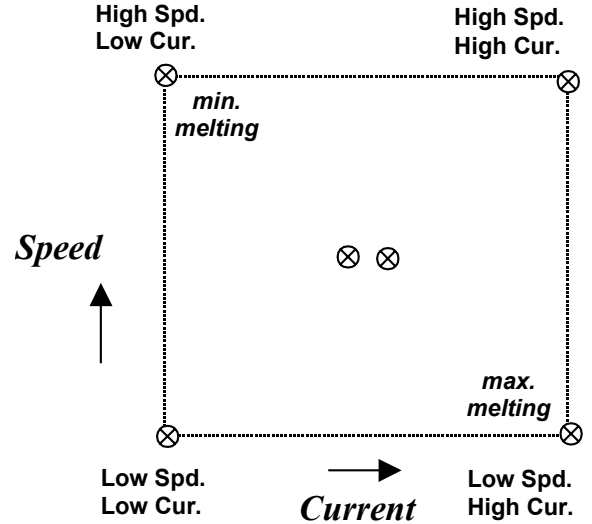


Fig. 1 Matrix of weld procedures used to obtain large range of weld conditions for experiment edge welds.

To help demonstrate the utility of these models for contrasting materials, dimensionless parameter correlations

were generated and compared with the actual experimental data. Equations 3-8 represent five useful dimensionless

$$Ry = \frac{q_i v}{\alpha^2 \delta h} \quad (3D) \quad (4)$$

$$Ro = \frac{q_i}{tk\Delta T} \quad (2D) \quad (5)$$

$$Ch = \frac{v^2 A}{\alpha^2} \quad (3D) \quad (6)$$

$$w^* = \frac{vA}{t\alpha} \quad (2D) \quad (7)$$

$$\eta_m = \frac{vA\delta h}{q_i} \quad (2D \& 3D) \quad (8)$$

parameters for analyzing conduction heat flow in fusion welding. Ry and Ro are dimensionless parameters first given by Rykalin⁷ and Rosenthal⁵ which are applicable for 3D heat flow and 2D heat flow respectively. Each can be considered heating parameters since they contain the input power in the numerator. Similarly Ch and w^* are dimensionless parameters that represent the weld size for 3D and 2D heat flow respectively. Ch is named after Christensen⁸ and w^* is often called dimensionless width. η_m represents the melting efficiency, which is the ratio of the power necessary to just melt the fusion zone to the net power absorbed by the part. It is an important figure of merit for a weld procedure. The maximum theoretical melting efficiency for 2D heat flow is 0.48, and 0.37 for 3D heat flow.

Results and Discussion

Numerical results of least squares fitting for thermal conductivity and thermal diffusivity are given in Table 1. As indicated, data sets with previous calorimeter measured input power were used for some materials. These sets serve as a comparison for welds where net input power has been accurately measured, and for the present experiment where net power is only estimated. The 3 values for thermal conductivity given for 304 stainless steel in Table 1 have a mean of 33.8 and a standard deviation of 3.9, which yields a $\pm 11.1\%$ variation in magnitude. This variation may be due to differences in experimental set-up, material chemistry, heat flow geometry, and perhaps the conduction model fit. Thermal property values for the other materials given in Table 1 may be expected to be similarly uncertain.

Figures 2-5 illustrate the correlations that were obtained between the dimensionless parameters and the 2D line source (2) equation. The 2D model is the same in each figure, the property fitting method simply adjusts the locations of the experimental data. The six experimental matrix welds used to characterize Kovar in Fig. 3 can be seen to correlate reasonably well with the model in each case. For Hastelloy B2, the experimental matrix did not produce a large change in Ro for the four welds grouped together in Fig. 4; as a result little variation in w_o was observed. As can be seen in Fig. 5, seven welds were used to fit 1100 aluminum to the conduction heat flow model and good variation in Ro was obtained. Similar fits to these have been made for each of the materials given in Table 1. To increase our confidence in the thermal property results, a larger range in Ro is in most cases

Table 1

Material	Liquidus Temperature (°C)	Effective Thermal diffusivity (mm ² /s)	Effective Thermal conductivity (W/mK)	Enthalpy of melting (J/mm ³)
304 SS (cal) ref. 2.	1454	6.3	38.4	8.7 ref. 2.
304 SS	1454	4.7	28.8	8.7
304 SS 3D (cal) ref. 3.	1454	5.6	34.3	8.7
Nickel 200 (cal) ref. 2.	1453	17.9	126	9.9*
Hastelloy C4	1397	8.3	60.0	9.9*
Hastelloy C22	1399	6.4	46.4	9.9*
Hastelloy B2	1431	7.2	50.6	9.9*
6061 aluminum	650	57.4	229	2.5*
1100 aluminum	660	59.8	237	2.5*
Kovar	1490	11.1	75.2	9.9*
HY 80 steel ref. 4.	1503	6.2	44	10.4 ref. 6.

*value for pure metal from ref.

Note: all values are from 2D model fits except where 3D fit indicated.

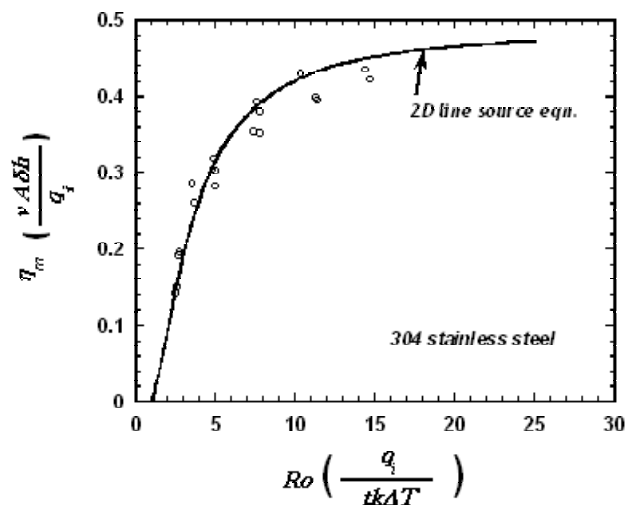


Fig. 2. Dependence of melting efficiency on the Rosenthal parameter for 304 stainless steel data taken from ref.2.

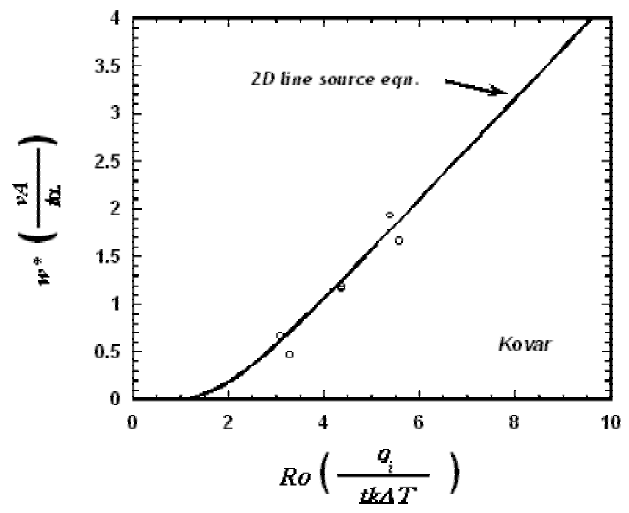


Fig. 3. Dependence of dimensionless weld width on the Rosenthal parameter for Kovar welds made in this experiment.

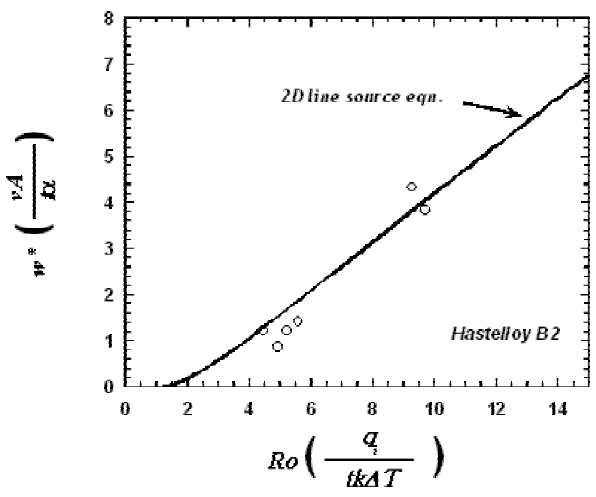


Fig. 4. Dependence of dimensionless weld width on the Rosenthal parameter for Hastelloy B2 welds made in this experiment.

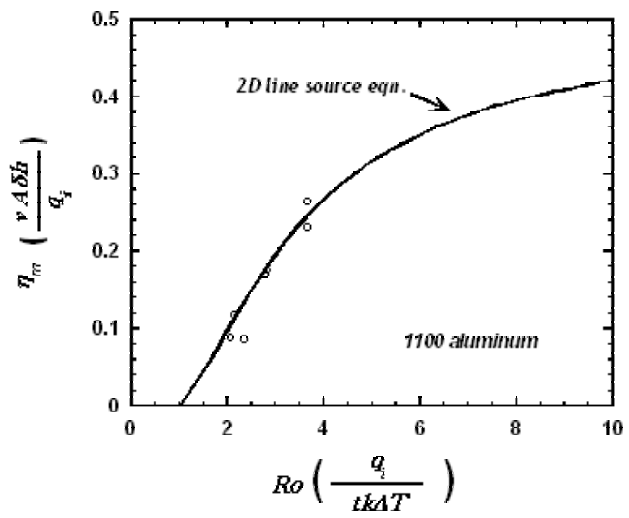


Fig. 5. Dependence of melting efficiency on the Rosenthal parameter for pure aluminum welds made in this experiment.

desirable: but it was not achievable with the thin section materials used in this experiment. One must consider that the simplicity of this experimental method is in part due to the ready availability of sheet metal specimens like those welded here. If larger samples, or more test welds are made, the cost of analysis will certainly increase.

This fitting method also applies to welds made on thick plates, since the 3D conduction heat flow equation for a semi-infinite plate can be employed to fit thick plate weld data. Two examples of data available in the open literature that were fit to the 3D model (3) are shown in Figs. 6 and 7. It is important to note that some of the dimensionless parameters given in Figs. 6 and 7 differ significantly from those in Figs. 2-5. But as in the 2D case, an acceptable correlation between the weld data and the conduction model can be readily obtained by fitting the thermal diffusivity to the model. Unique to these two data sets in the literature was a listing of weld cross-sectional area measurements. As mentioned earlier, accurate correlations with these fitting methods require careful characterization of fusion zone melting that can only be

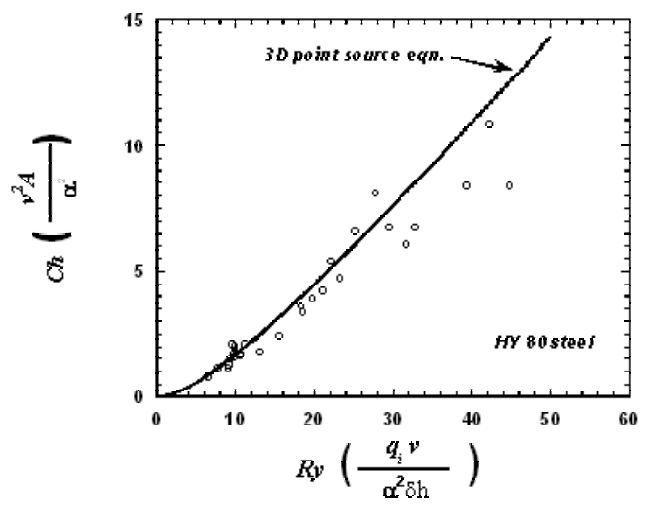


Fig. 6. Dependence of the Christensen parameter on the Rykalin parameter for HY 80 steel thick plate welds from ref.4.

obtained with cross-section area data.

Since both the 2D and 3D correlations are based in theory and are validated on real materials, extrapolation beyond the parameter levels used in the experiments is certainly valid and an important benefit of this methodology. The availability of welding models like these is critical to the application of automatic welding and to increased understanding of the science of welding. Refinements to these models will surely improve their predictive capability, but until manufacturers begin to apply these methods on the production floor, little progress can be expected. It is hoped that the recent incorporation of these thermal property values into desktop software by the authors⁹ will lead to increased application of welding models in industry, and their continued improvement into routine production tools.

Conclusions

1. 2D and 3D moving heat source solutions to the conduction heat flow equation were used to estimate the thermal diffusivity and thermal conductivity of nine engineering alloys.
2. Dimensionless parameter correlations for these solutions were given and enabled a direct comparison between the welded material results and the conduction theory.
3. The property estimations have been shown to agree to within $\pm 11.1\%$ for 304 stainless steel welds that were made under contrasting experimental conditions.
4. The least squares fitting method employed has also been applied to data sets in the open literature for 3D heat flow and found to be similarly effective.

Acknowledgments

The authors wish to thank Alice Kilgo, Chris Morgan, and Fred Hooper for their important assistance during the completion of this paper. This work was performed at Sandia National Laboratories. Sandia is a multiprogram laboratory operated by Sandia Corporation, a Lockheed Martin Company, for the U.S. Dept of energy under contract number DE-AC04-94A185000.

References

1. Rosenthal, D. & Friedman, N. E. *The Determination of Thermal Diffusivity of Aluminum Alloys at Various Temperatures by Means of A Moving Source*. *Trans. ASME* **78**, 1175-80 (1956).
2. Fuerschbach, P. W. & Knorovsky, G. A. *A Study of Melting Efficiency in Plasma Arc and Gas Tungsten Arc Welding*. *Welding Journal* **70**, 287s-297s (1991).
3. Giedt, W. H., Tallerico, L. N. & Fuerschbach, P. W. *GTA Welding Efficiency: Calorimetric and Temperature Field Measurements*. *Welding Journal* **68**, 28s-32s (1989).
4. Niles, R. W. & Jackson, C. E. *Weld Thermal Efficiency of the GTAW Process*. *Welding Journal* **54**, 25s-32s (1975).
5. Rosenthal, D. *The Theory of Moving Sources of Heat and Its Application to Metal Treatments*. *Transactions of the ASME*, 849-866 (1946).
6. Kelley, K. K. *Contributions to the Data on Theoretical Metallurgy (U.S. Bureau of Mines, Washington, D.C., 1960)*.
7. Rykalin, N. N. *Calculation of Heat Flow in Welding (Translated by Zvi Paley and C. M. Adams Jr., Moscow, 1951)*.
8. Christensen, N., Davies, V. L. & Gjermundsen, K. *Distribution of Temperatures in Arc Welding*. *British Welding Journal* **12**, 54-75 (1965).
9. Fuerschbach, P. W. & Eisler, G. R. *in Science Based Weld Software to Develop Optimal Automatic Welding Procedures (Sandia National Laboratories, 2002)*.